ZEUS-prel-05-025-updated

Submitted to the
33nd International Conference oh High Energy Physics
July 26 – August 2, 2006; Moscow, Russia

Session: QCD hard interactions

Photoproduction of Events with Rapidity Gaps between Jets at HERA

ZEUS Collaboration

17th July 2006

Abstract

Cross sections for the photoproduction of dijet events, where the two jets with the highest transverse energy are separated by a large gap in pseudorapidity, have been studied with the ZEUS detector using an integrated luminosity of 38.6 pb^{-1}. Rapidity-gap events are defined in terms of the energy flow between the jets, such that the total summed transverse energy in this region is less than some value $E_{\mathrm{T}}^{\mathrm{CUT}}$. The data show a clear excess above the predictions of standard photoproduction models. Models which include color-singlet exchange are able to describe the data.

1 Introduction

The production of events in hadronic collisions with two high transverse energy jets in the final state separated by a large rapidity interval provides an ideal environment to study the interplay between soft, non-perturbative and hard, perturbative QCD.

The dominant mechanism for the production of jets with high transverse energy in hadronic collisions is a hard interaction between partons in the incoming hadrons via a quark or gluon propagator. The exchange of colour quantum numbers generally gives rise to jets in the final state that are colour connected to each other and the remnants of the incoming hadrons. This leads to energy flow which populates the pseudo-rapidity region both between hadronic remnants and the jets themselves. Events with a large rapidity interval and little or no hadronic activity between the jets would then be a signature of the exchange of a colour singlet object.

The presence of high transverse energy jets provides a perturbative hard scale at each end of the colour singlet exchange, such that the cross section should be fully calculable in perturbative QCD [1].

Previous studies of jets with rapidity gaps have been made in $p\bar{p}$ collisions at the Tevatron [2, 3] and in photoproduction at HERA [4, 5]. Comparison with different Monte Carlo (MC) models suggested that some contribution of color-singlet exchange may be required to describe the data, although the uncertainty on the contribution from standard QCD processes was large.

In the current analysis, photoproduction of dijet events with a large rapidity separation between jets, defined as in the recent publication of H1 collaboration [5], is used to investigate the dynamics of color singlet exchange. With much more statistics and MC models, tuned to better describe the data sample at the detector level, the color-singlet contribution is studied and compared to available models.

2 Data selection

The results presented in this paper correspond to 38.6 $\pm$ 1.6 pb^{-1} of data taken with the ZEUS detector during the 1996-1997 HERA running period. Positrons of 27.5 GeV collided with protons of 820 GeV, giving a center of mass energy of $\sqrt{s} = 300\,\text{GeV}$.

A three-level trigger system was used to select events online [6,7]. In the third-level trigger, jets were required to have a transverse energy of $E_{\rm T}^{jet} > 4\,\text{GeV}$ and a pseudorapidity of $\eta^{jet} < 2.5$ in the laboratory frame.

The kinematic variables, y (inelasticity) and W (the γp center-of-mass energy), were reconstructed using the Jacquet-Blondel (JB) [8] method. The sums were run over all Energy Flow Objects (EFOs), which were formed by combining information from energy clusters reconstructed in the CAL and charged tracks reconstructed in the CTD [9]. The electron (e) reconstruction method was also used for cleaning cuts.

The photoproduction sample was selected by applying the following cuts offline:

- the longitudinal position of the reconstructed vertex was required to be in the range $-40\,\text{cm} < Z_{vertex} < 40\,\text{cm}$ in order to reduce contributions from beam-gas interactions, cosmic-ray showers, and beam-halo muons;
- events with a scattered positron in the CAL having $y_e < 0.85$ and $E'_e > 5\,\text{GeV}$, where E'_e is the energy of the scattered positron, were rejected. This cut reduced contamination from neutral current DIS events in a region where efficiency for the scattered positron to be detected approached 100%;
- events were required to have $0.2 < y_{JB} < 0.75$. The upper cut on y_{JB} further reduced contamination from the neutral current DIS events which were not removed by the cut on y_e and the lower cut removed beam-gas events;
- events were required to have a relative transverse momentum $p_T/\sqrt{E_T} < 2.0\,\text{GeV}^{1/2}$ in order to reduce the contribution of charged current events and further reduce the contribution from cosmic-ray showers.

The cuts on y_e and y_{JB} reduced the contribution of DIS events to less than 0.5% and restricted the photon virtuality to a range of $Q^2 < 1\,\text{GeV}^2$ with a median value of $Q^2 \sim 10^{-3}\,\text{GeV}^2$ [10].

Jets were reconstructed from the EFOs using the k_T algorithm [11] in the longitudinally invariant inclusive mode [12] and ordered in E_{T}. Events in which jets satisfied the following criteria were then selected:

- $E_{\mathrm{T}}^{jet1} \geq 5$ GeV and $E_{\mathrm{T}}^{jet2} \geq 4.25$ GeV, where E_T^{jet1} and E_T^{jet2} are the transverse energy of the corresponding jets. This cut corresponds to the $E_{\mathrm{T}}^{jet1} \geq 6$ GeV and $E_{\mathrm{T}}^{jet2} \geq 5$ GeV at the hadron level;
- $-2.4 < \eta^{jet1,2} < 2.4$, where η_1 and η_2 are the pseudorapidities of the corresponding jets, to ensure that the jets were well constructed in the CAL;
- $2.5 < \Delta\eta < 4$, where $\Delta\eta \equiv |\eta^{jet1} - \eta^{jet2}|$ is the absolute difference in pseudorapidity between the jets;
- $\frac{1}{2}|\,(\eta^{jet1} + \eta^{jet2})\,| < 0.75$, this condition together with the previous one constrain the jets to lie within the kinematic region where the detector and event simulation are best understood.

The transverse energy in the gap, $E_{\rm T}^{\rm GAP}$, was calculated by summing up the transverse energy of all jets, without any cut on $E_{\rm T}$. lying in the pseudorapidity region between the two highest-$E_{\rm T}$ jets satisfying the above requirements [13]. Gap events were defined as those in which $E_{\rm T}^{\rm GAP}$ was less than an $E_{\rm T}^{\rm CUT}$ value, where the $E_{\rm T}^{\rm CUT}$ values used in this analysis were $E_{\rm T}^{\rm CUT} = 0.5, 1.0, 1.5$, and $2.0\,{\rm GeV}$. The gap fraction, f, was defined as the ratio of the cross section for gap events to the cross section for inclusive events, which pass all of the above cuts but have no restriction on the $E_{\rm T}^{\rm GAP}$ value.

In addition, the fraction of the photon momentum carried by a parton participating in the hard interaction was calculated as $x_\gamma^{\rm OBS} = (E_{\rm T}^{\rm jet1} e^{-\eta^{\rm jet1}} + E_{\rm T}^{\rm jet2} e^{-\eta^{\rm jet2}})/2yE_e$, where E_e is energy of initial lepton.

3 Monte Carlo simulations

The Pythia 6.1 [14] and Herwig 6.1 [15] MC generators were used to correct the data to the hadron level and for model comparisons. Both MCs are based on the leading order (LO) ($2 \rightarrow 2$) matrix elements together with a parton-shower simulation of additional QCD radiation and hadronisation models.

In photoproduction interactions at leading order the photon can either interact directly in the hard sub-process (direct photoproduction) or first fluctuate into a hadronic state and then interact via a partonic constituent carrying some fraction, x_γ, of the photon momentum (resolved photoproduction). At leading order, therefore, color-singlet exchange may take place only in resolved photoproduction. For this analysis the direct, resolved, and color-singlet exchange Monte Carlo samples were generated separately.

The simulation of multi-parton interactions was included in Pythia using the simplest MPI available option[1] and in Herwig by interfacing to the Jimmy library [16]. The minimum transverse momenta, $p_{\rm T}^{\rm min}$, of the outgoing partons in the hard interaction and MPIs are separately adjustable in Pythia, while in Herwig the same parameter was used to adjust both momenta. The $p_{\rm T}^{\rm min}$ was tuned for both MC programs by comparisons to the data sample after the kinematic cuts were applied (see Section 2). The $p_{\rm T}^{\rm min}$ values used in this analysis were $p_{\rm T}^{\rm min1} = 1.9\,{\rm GeV}$ and $p_{\rm T}^{\rm min2} = 1.7\,{\rm GeV}$ for Pythia and $p_{\rm T}^{\rm min} = 2.7\,{\rm GeV}$ for Herwig. The tuning of $p_{\rm T}^{\rm min}$, as well as other parameters, was influenced by the global fits of JetWeb [17].

The color-singlet exchange is implemented in Herwig using the LLA BFKL model by Mueller and Tang [18]. The hard-Pomeron intercept, $1 + \omega_0$, is related to the strong cou-

[1] Multiparton interactions in Pythia were selected by setting MSTP(82)=1

pling, α_s, along the gluon ladder in the BFKL parton evolution by $\omega_0 = \alpha_s C_A [4 \ln (2/\pi)]$. In this analysis, the default values of $\alpha_s = 0.17$ and $\omega_0 = 0.3$ were used.

PYTHIA does not contain a simulation of strongly interacting color-singlet exchange in hard interactions. However, an event topology similar to that of color-singlet exchange can be simulated by high-t photon exchange for quark-quark scattering in leading-order (LO) resolved processes. Such an exchange is only used to compare the data and MC predictions and is not expected to describe the mechanism of color-singlet exchange.

Hadronisation in HERWIG is simulated using the cluster model [19] while PYTHIA uses Lund string model [20].

The data were corrected to the hadron level with a bin-by-bin method using a combination of direct, resolved, and color-singlet MC samples.

4 Results

The inclusive dijet cross section as a function of $E_{\mathrm{T}}^{\mathrm{GAP}}$ is presented in Fig. 1. At low $E_{\mathrm{T}}^{\mathrm{GAP}}$ values, where the color-singlet contribution should be most pronounced, the data demonstrates a clear rise towards the small $E_{\mathrm{T}}^{\mathrm{GAP}}$ values. In order to estimate the amount of the color singlet, the direct and resolved components of each MC were mixed according to their cross sections, as predicted by the MC, to give the color-non-singlet MC sample. The color-non-singlet and color-singlet MC samples were then fitted to the data. The best fit to the data resulted in multiplicative scaling parameters 426 for PYTHIA and 1.45 for HERWIG CS contributions. These scaling parameters were used in this analysis when comparing data to the MC predictions. The amount of the color singlet contribution to the total cross section, estimated by integrating the MC predictions over the entire $E_{\mathrm{T}}^{\mathrm{GAP}}$ range, was found to be in the region $2-3\%$ for both PYTHIA and HERWIG.

The inclusive dijet cross section, the gap cross section, and the gap fraction, as a function of the separation, $\Delta\eta$, of the two leading jets, are presented in Fig. 2. for $E_{\mathrm{T}}^{\mathrm{CUT}} = 1\,\mathrm{GeV}$. Both cross sections and the gap fractions decrease as a function of $\Delta\eta$. In the inclusive cross section, both MC models with and without color-singlet exchange describe the data equally well, but for the gap cross section, the MC models without color-singlet exchange fall below the data while the MC models with color-singlet exchange describe the data. The contribution of color-singlet exchange to the total gap fraction increase as the dijet separation increases from 2.5 to 4 units in pseudorapidity.

Figure 3 shows the gap fraction as a function of the dijet separation, $\Delta\eta$, for the four values of $E_T^{\mathrm{CUT}} = 0.5, 1.0, 1.5$ and $2\,\mathrm{GeV}$. The data first fall and then level out as $\Delta\eta$ increases for all values of E_T^{CUT} except $E_T^{\mathrm{CUT}} = 0.5$, where the data is almost constant with

$\Delta\eta$. The predictions of PYTHIA and HERWIG without color-singlet exchange lie below the data over the entire $\Delta\eta$ range. With the addition of the color-singlet contribution both MCs describe the data well. These results agree within uncertainties with the previous H1 measurement [5], where the gap definition used the transverse energy in the gap as for the current analysis, but with slightly different kinematic cuts.

In order to estimate the color-singlet contribution to the gap fraction, the data were compared to the MC predictions as shown in Fig. 3. The color-singlet contribution differs, depending on the MC used in the comparison, and increasing slightly with increasing $\Delta\eta$.

For comparison with other experiments and *pp* measurements, the cross sections and gap fraction were also measured as function of x_γ^{OBS}. These results are presented in Fig. 4 for four different values of $E_\mathrm{T}^{\mathrm{CUT}}$. The gap fraction increases as a function of x_γ^{OBS} and the data are reasonably described by both MC models. In the x_γ^{OBS} region below 0.75 HERWIG predicts larger cross sections than PYTHIA. Although the data have sufficiently small errors, the difference in the models predictions preclude an accurate determination of the color-singlet contribution to the gap fraction and its behavior as a function of x_γ^{OBS}.

In order to compare with *pp* measurements the $\Delta\eta$ behavior was investigated in the resolved enhanced region. Figure 5 shows the gap fractions as function of $\Delta\eta$ for the resolved enhanced sample for the four $E_\mathrm{T}^{\mathrm{CUT}}$ values. For $E_\mathrm{T}^{\mathrm{GAP}} < 0.5\,\mathrm{GeV}$ and $E_\mathrm{T}^{\mathrm{GAP}} < 1.0\,\mathrm{GeV}$, both MC models predict almost no contribution to the gap fractions from the non-color-singlet component at high values of $\Delta\eta$. These points are therefore less biased by the model predictions and can be used to estimate the color-singlet contribution in the resolved enhanced sample.

5 Summary

The analysis of cross sections of dijet photoproduction events, where the two jets with the highest transverse energy are separated by a large region in pseudorapidity and have very little transverse energy between them, show a clear excess when compared to the predictions of standard photoproduction MC models. The same models, with the inclusion of a color-singlet exchange sample on the level of $2-3\%$, are able to describe the data. The same amount of color-singlet exchange is observed by direct comparison of the data to the MC predictions using the gap fractions.

References

[1] J.R. Forshaw and P.J. Sutton, Eur. Phys. J. **C 1**, 285 (1998).

[2] DØ Coll. B. Abachi et al., Phys. Rev. Lett. **72**, 2332 (1994);
DØ Coll. B. Abachi et al., Phys. Rev. Lett. **76**, 734 (1996);
DØ Coll. B. Abbott et al., Phys. Lett. **440**, 189 (1998).

[3] CDF Coll., F. Abe et al., Phys. Rev. Lett. **74**, 855 (1995);
CDF Coll., F. Abe et al., Phys. Rev. Lett. **80**, 1156 (1998);
CDF Coll., F. Abe et al., Phys. Rev. Lett. **81**, 5278 (1998).

[4] ZEUS Coll., M. Derrick et al., Phys. Lett. **B 369**, 55 (1996).

[5] H1 Coll., C. Adloff et al., Eur. Phys. J. **C 24**, 517 (2002).

[6] ZEUS Coll., U. Holm (ed.), *The ZEUS Detector*. Status Report (unpublished), DESY (1993), available on `http://www-zeus.desy.de/bluebook/bluebook.html`.

[7] ZEUS Coll., J. Breitweg et al., Z. Phys. **C 74**, 207 (1997).

[8] F. Jacquet and A. Blondel, *Proceedings of the Study for an ep Facility for Europe*, U. Amaldi (ed.), p. 391. Hamburg, Germany (1979). Also in preprint DESY 79/48.

[9] N. Harnew et al., Nucl. Inst. Meth. **A 279**, 290 (1989);
B. Foster et al., Nucl. Phys. Proc. Suppl. **B 32**, 181 (1993);
B. Foster et al., Nucl. Inst. Meth. **A 338**, 254 (1994).

[10] S. Chekanov, et al., Eur. Phys. J. **C23**, 615 (2002).

[11] S.Catani et al., Nucl. Phys. **B406**, 187 (1993).

[12] S.D. Ellis and D.E. Soper, Phys. Rev. **D 48**, 3160 (1993).

[13] G. Oderda and G. Sterman, Phys. Rev. Lett. **81**, 3591 (1998).

[14] T. Sjöstrand, Comp. Phys. Comm. **82**, 74 (1994).

[15] G. Marchesini et al., Comp. Phys. Comm. **67**, 465 (1992).

[16] J.M. Butterworth, J.R. Forshaw and M. Seymour, Z. Phys. **C 72**, 637 (1996).

[17] J.M. Butterworth and S.Butterworth, Comput. Phys. Commun. **153**, 164 (2003).

[18] A.H. Mueller and W.K. Tang, Phys. Lett. **B 284**, 123 (1992).

[19] G. Marchesini, B.R. Webber, Nucl. Phys. **B 310**, 461 (1988).

[20] B. Andersson et al., Phys. Rep. **97**, 31 (1983).

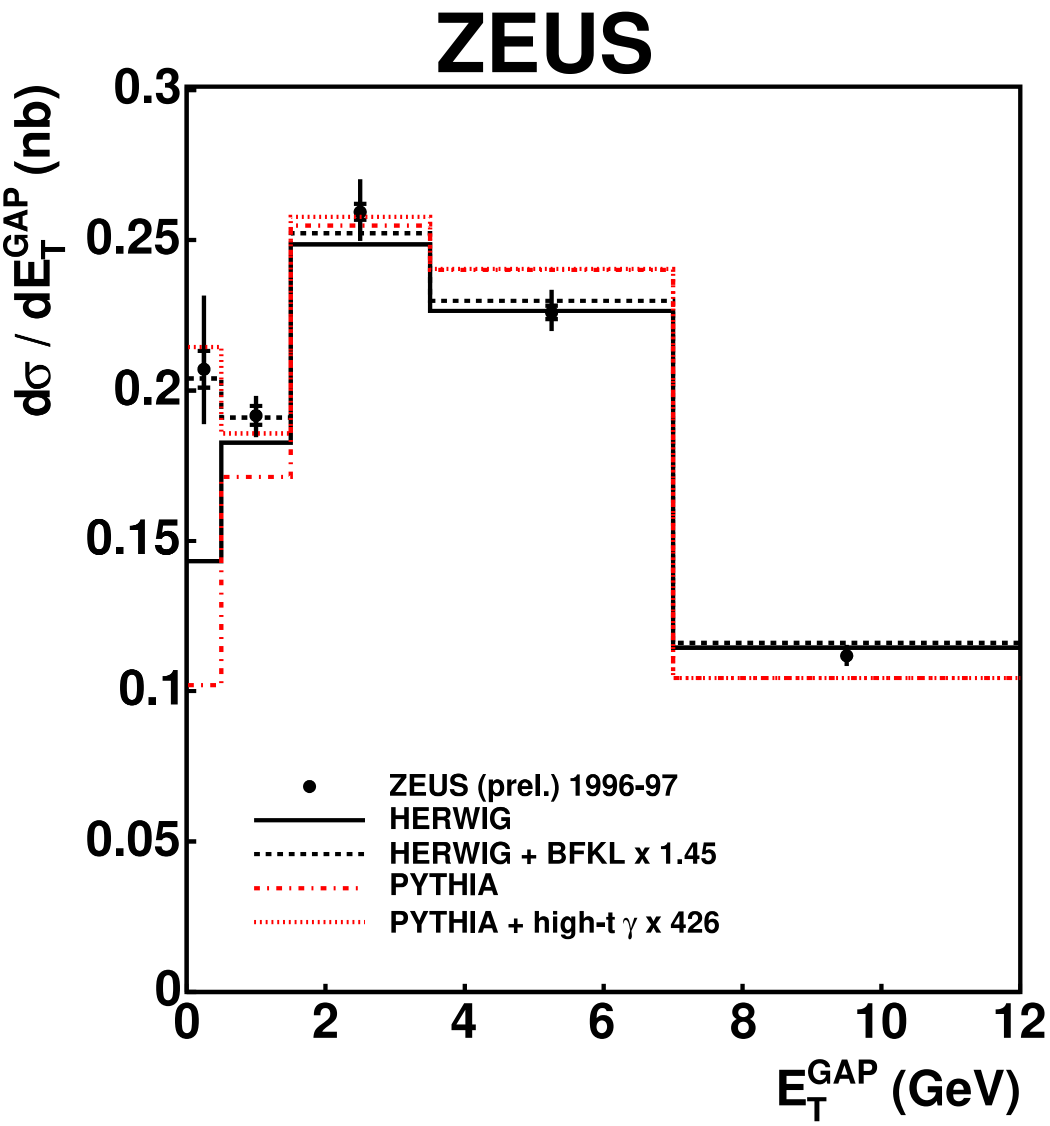

Figure 1: *The inclusive dijet cross section differential in E_T^{GAP}. The black circles represent the ZEUS data, with the inner error bars representing the statistical errors and the outer error bars representing the statistical and systematic uncertainties added in quadrature. The solid black line shows the prediction of* HERWIG *and the black dashed line shows the prediction of* HERWIG *plus* BFKL *Pomeron exchange. The dot-dashed line shows the prediction of* PYTHIA *and the dotted line shows the prediction of* PYTHIA *plus high-t photon exchange. The band shows the calorimeter energy scale uncertainty.*

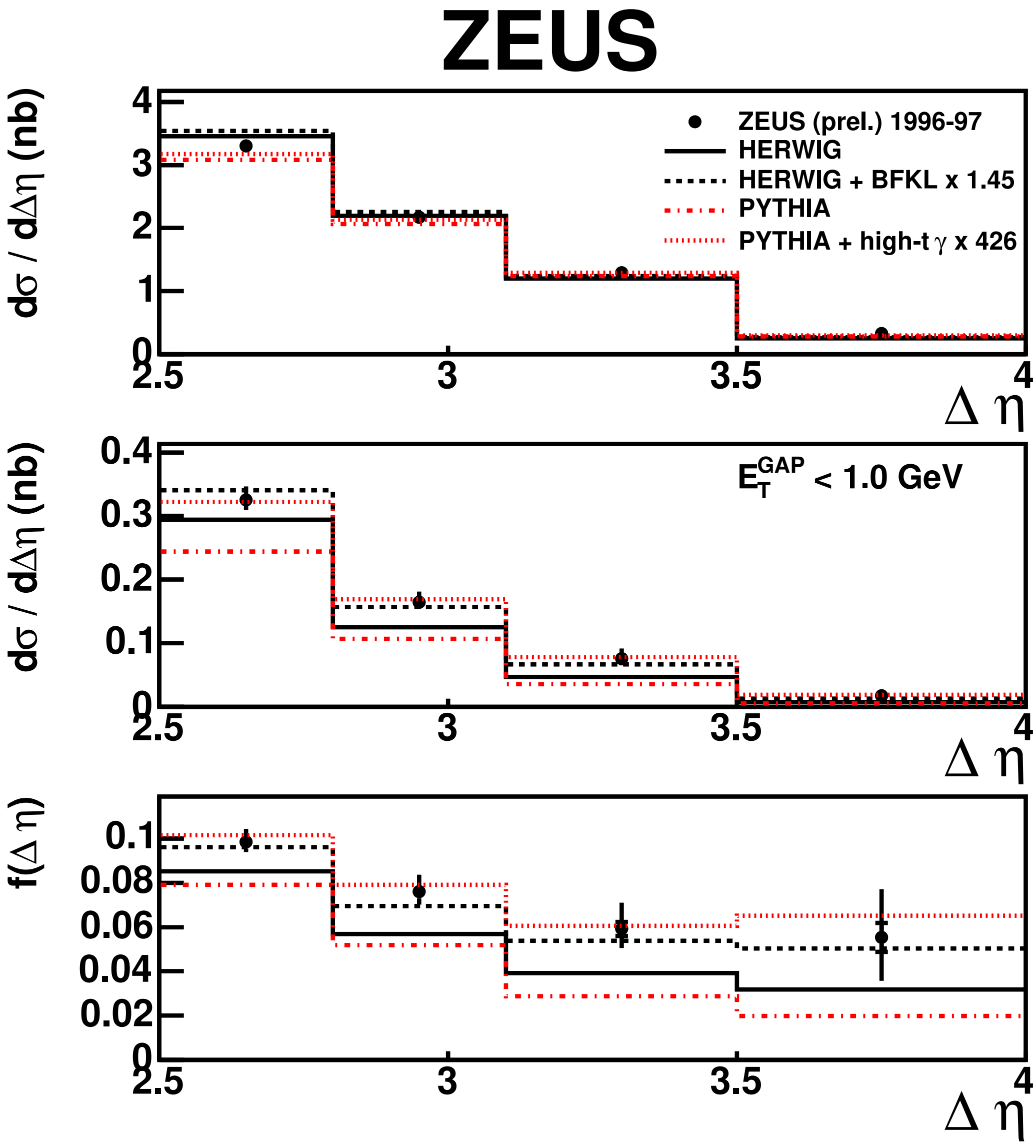

Figure 2: *The top plot is the inclusive dijet cross section differential in $\Delta\eta$, The middle plot is the gap cross section differential in $\Delta\eta$ requiring that $E_{\mathrm{T}}^{\mathrm{GAP}} < 1$ GeV, and the bottom plot is the gap fraction, f, in $\Delta\eta$. The black circles represent the ZEUS data, with the inner error bars representing the statistical errors and the outer error bars representing the statistical and systematics uncertainties added in quadrature. The solid black line shows the prediction of* HERWIG *and the black dashed line shows the prediction of* HERWIG *plus* BFKL *Pomeron exchange. The dot-dashed line shows the prediction of* PYTHIA *and the dotted line shows the prediction of* PYTHIA *plus high-t photon exchange. The band shows the calorimeter energy scale uncertainty.*

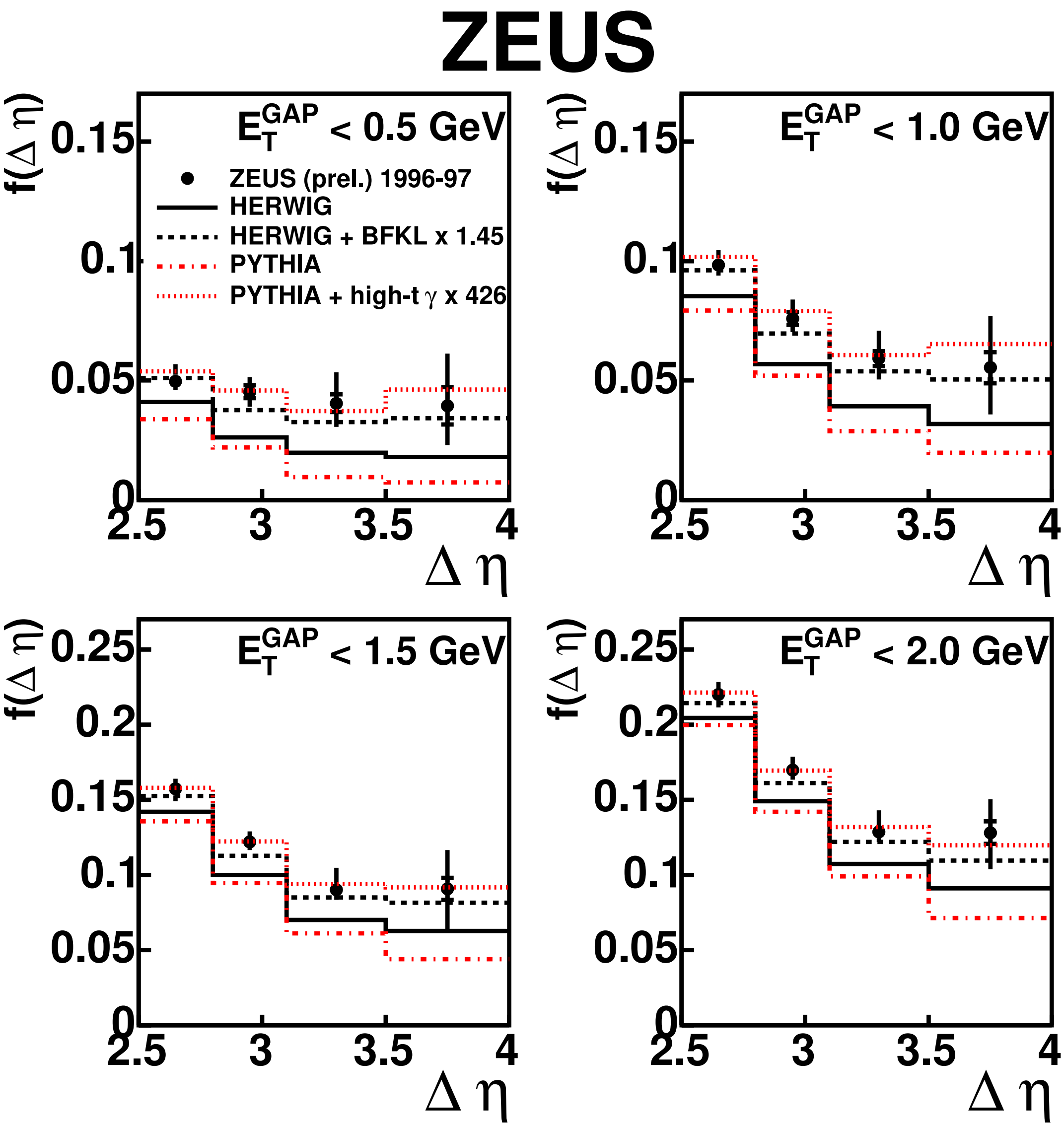

Figure 3: *The gap fraction, f, in $\Delta\eta$. The black circles represent the ZEUS data, with the inner error bars representing the statistical errors and the outer error bars representing the statistical and systematics uncertainties added in quadrature. The solid black line shows the prediction of* HERWIG *and the black dashed line shows the prediction of* HERWIG *plus* BFKL *Pomeron exchange. The dot-dashed line shows the prediction of* PYTHIA *and the dotted line shows the prediction of* PYTHIA *plus high-t photon exchange. The band shows the calorimeter energy scale uncertainty.*

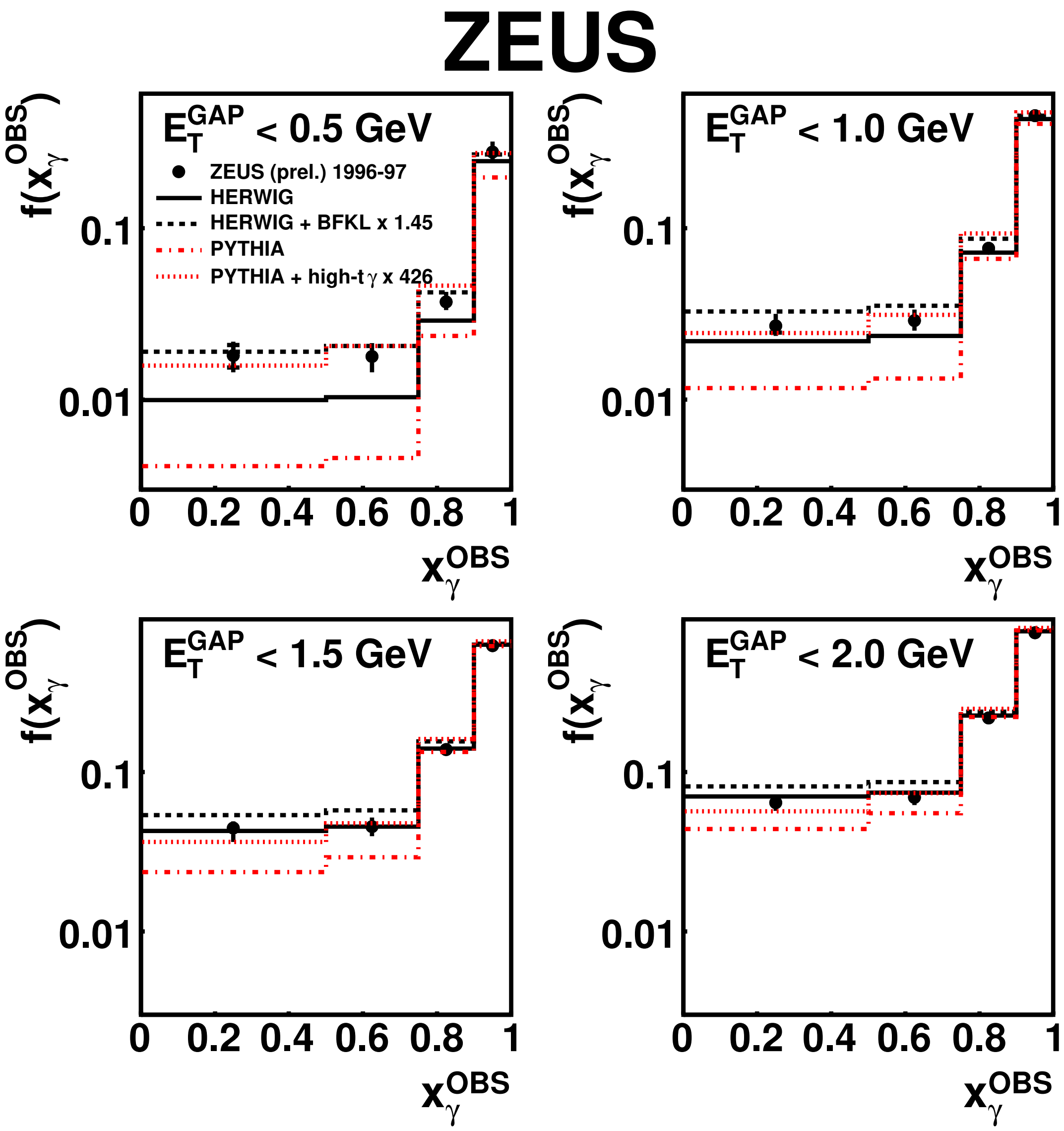

Figure 4: *The gap fraction, f, in $x_\gamma^{\rm OBS}$. The black circles represent the ZEUS data, with the inner error bars representing the statistical errors and the outer error bars representing the statistical and systematics uncertainties added in quadrature. The solid black line shows the prediction of* HERWIG *and the black dashed line shows the prediction of* HERWIG *plus* BFKL *Pomeron exchange. The dot-dashed line shows the prediction of* PYTHIA *and the dotted line shows the prediction of* PYTHIA *plus high-t photon exchange. The band shows the calorimeter energy scale uncertainty.*

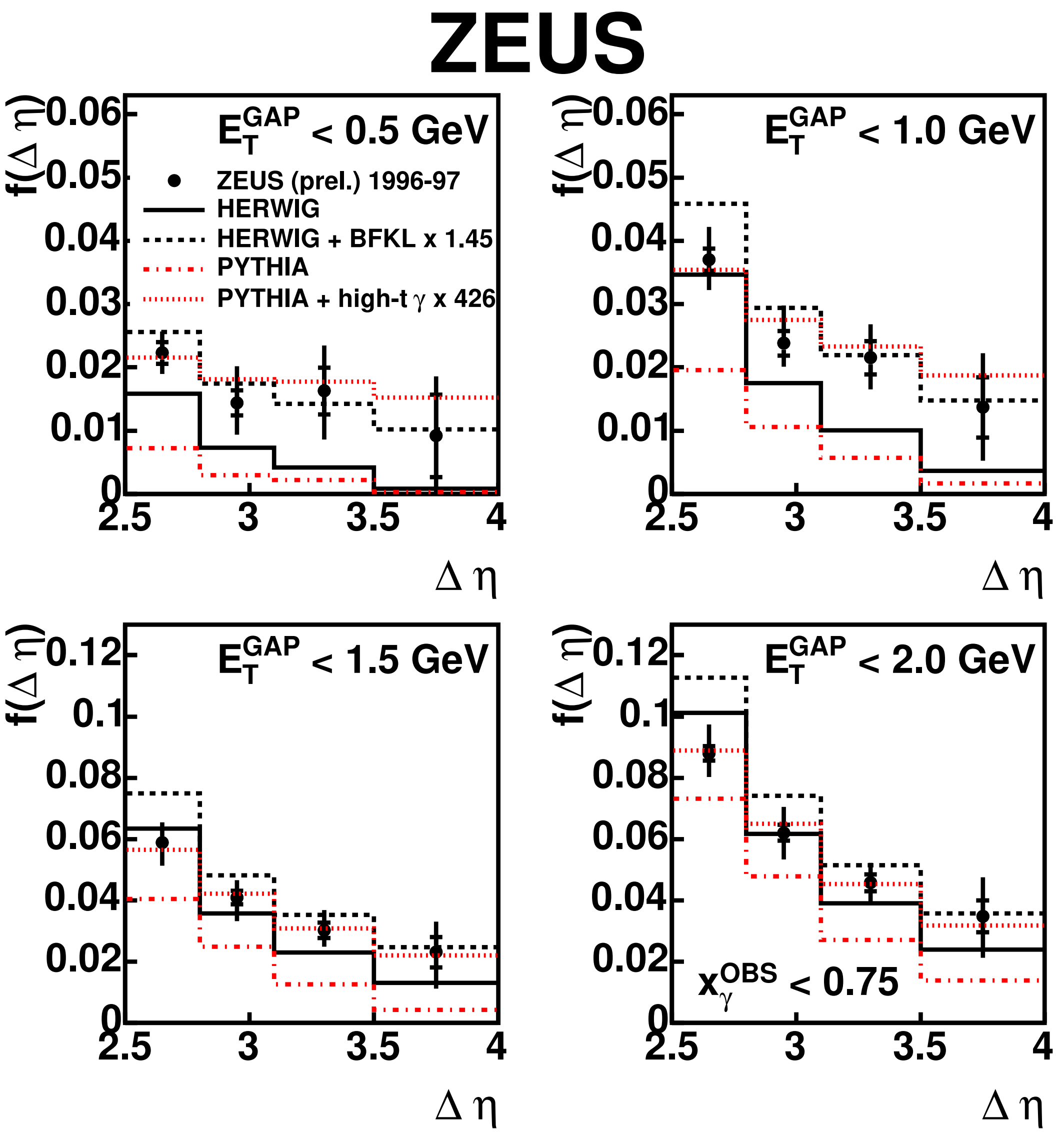

Figure 5: *The gap fraction, f, in $\Delta\eta$ for $x_\gamma^{\rm OBS} < 0.75$. The black circles represent the ZEUS data, with the inner error bars representing the statistical errors and the outer error bars representing the statistical and systematics uncertainties added in quadrature. The solid black line shows the prediction of* HERWIG *and the black dashed line shows the prediction of* HERWIG *plus* BFKL *Pomeron exchange. The dot-dashed line shows the prediction of* PYTHIA *and the dotted line shows the prediction of* PYTHIA *plus high-t photon exchange. The band shows the calorimeter energy scale uncertainty.*